JOURNAL OF COMPUTATIONAL PHYSICS 54, 3–17 (1984)

Short Period Seismology

KEIITI AKI

Department of Earth and Planetary Sciences,
Massachusetts Institute of Technology, Cambridge, Massachusetts 02139

Received June 15, 1981

Short period seismology is in a transition period from the 1-D earth model (in which properties vary only with depth) to the 3-D model. Theory and methods are well established for the 1-D model. The methods for handling the travel time data using the 3-D model have been developed recently for both forward and inverse problems. The methods for wave forms and spectra in the 3-D model are still in a rudimentary stage. Stochastic approaches in earth structure modeling are useful particularly for short period waves for which the data are usually not sufficient for a deterministic interpretation.

INTRODUCTION

Since this paper is addressed to an audience of mathmaticians and seismologists, it is appropriate to begin with a few equations.

$$\rho \ddot{u}_i = f_i + \tau_{ij,j}, \tag{1}$$

$$\tau_{ij} = c_{ijpq} e_{pq}, \tag{2}$$

$$W = 1/2 c_{ijpq} e_{ij} e_{pq}. \tag{3}$$

These are the three most basic equations of seismology. Almost everything in theoretical seismology has been deduced from these three equations.

Equations (1) and (2) originate from Newton and Hooke, respectively, as is well known. Less well known is the fact that these two great men were contemporaries in 17th century England but not very friendly to each other. Hooke believed that Newton stole his idea about the inverse square law on gravitational force. In any case, we owe them the origin of dynamic elasticity.

Of course, the concepts of stress components τ_{ij} and strain components e_{ij} were unknown in the 17th century. They were developed by Cauchy in the 1820s. The 1820s in France was an extraordinary period for elasticity theory. Fresnel explained various polarization effects of light by considering light to be a transverse elastic wave propagating through ether. Earlier, only a longitudinal wave was considered to propagate through the interior of a body. Poisson then showed that two types of waves which we now call P and S waves can propagate in the Newtonian atomic

0021-9991/84 $3.00

structure and that the ratio of the P wave velocity to S wave velocity is $\sqrt{3}$. Thus, the elastic waves played a central part in fundamental physics of this period.

With the introduction of stress and strain components, Cauchy founded the elasticity theory almost in the present day form, except for the concept of strain energy function W shown in Eq. (3). When Green put the foundation of elasticity on the existence of strain energy function in the middle of the 19th century, the basis for development of theoretical seismology was well prepared.

The First Observed and Synthetic Seismograms

The beginning of modern observational seismology took place in Japan in the early 1880s by British scientists and engineers who were teaching at the Imperial College of Tokyo. Milne was their leader and organized the first seismological society in the world. In fact, this year (1981) marks the centennial of the birth of a seismogram. The first published record of ground motion as a function of time is shown in Fig. 1. This is an earthquake near Tokyo on March 8, 1881 registered on a revolving smoked glass plate by a pair of horizontal pendulums (oriented East–West and North–South) designed by Ewing. In the middle of the figure, the first 20 sec of two-component records are shown on a common time-scale. It is clear that the first wave group is followed by a distinct arrival of the second one at about 10 sec from the

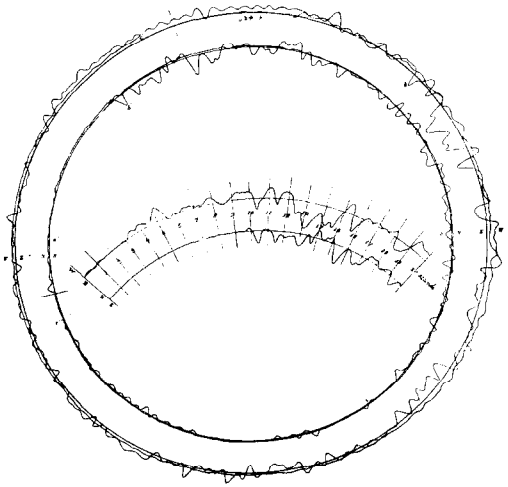

FIG. 1. A record, obtained with Ewing's horizontal pendulum seismograph, of a strong local earthquake on March 8, 1881 (reproduced from *Nature* **30** (1884), 174). Two of the pendulums write on the same surface. The recording plate revolves continuously and is stopped after an earthquake. The beginning of the earthquake is marked as a, a' (about 90° apart) respectively, on the EW and NS traces. In the center, the traces have been aligned on a common time scale.

onset. The first wave was called the P wave because it was the primary arrival, and the second one was called the S wave because it was the secondary arrival. Ewing correctly identified P waves as compressional waves and S waves as shear waves. Milne, however, disagreed with Ewing on the basis of observed polarization in relation to inferred direction of wave approach. This confusion about P and S waves lasted for more than 30 years because of the complexity of short-period waves from local earthquakes.

The identification of various wave types was much easier for distant earthquakes because the deeper earth through which the body wave travelled is more homogeneous, and also short-period waves, which are the source of complexity, are attenuated after they travel over a long distance. The first recording of a distant earthquake was made by Rebeur-Paschwitz in 1889 by a horizontal pendulum located at Potsdam which successfully recorded an earthquake in Japan.

In 1900, Oldham constructed the first travel time curve (a plot of arrival time as a function of distance from the epicenter measured along the Earth's surface) for distant earthquakes and correctly identified P, S, and surface waves. In order to draw a travel time curve, one must know the origin time and epicenter of an earthquake in addition to the arrival times at various places around the world. He was able to do so for the great Assam earthquake of 1897, because he made a detailed field study of the epicentral area after the earthquake and had the firsthand information about the epicenter and origin time.

The first synthetic seismogram, on the other hand, was computed by Lamb in 1904 for a point force buried in a homogeneous, isotropic elastic half-space. As shown in Fig. 2, it is much simpler than the first observed seismogram shown in Fig. 1. The difference was so great that it took a long time before experimental and theoretical seismologists started to talk to each other.

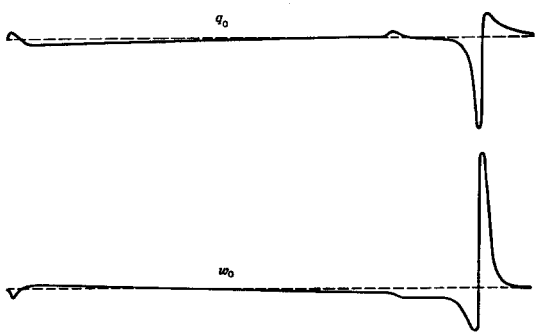

FIG. 2. The first synthetic seismogram due to Lamb (1904) for a point force in a homogeneous half space. Upper and lower curves are horizontal and vertical displacements, respectively.

Successful Comparisons between Observed and Synthetic Seismograms

The first successful comparison between the synthetic and experimental seismograms did not take place until 1948. The experimental seismogram was the acoustic waves in an ocean recorded by Ewing and Worzel, and the synthetic seismogram was computed by Pekeris as shown in Figs. 3 and 4, respectively, [1]. The synthetic seismograms for solid earth were first obtained in 1960 for Rayleigh and Love waves. Figure 5 shows a comparison of observed and synthetic Rayleigh waves across the United States from California to the east coast made by Aki [3] who used for the first time Lamb's result (more than a half century after its publication) in an interpretation of the initial phases of Rayleigh waves from actual earthquakes.

The first successful computation of synthetic seismograms for refraction experiments was made by Helmburger [4] in 1968 using the Cagniard–DeHoop method [11]. Figure 6 shows the comparison of the observed records (with time marklines at 0.1 sec interval) with the synthetic records (without time mark). The latter were computed for the crustal model with P and S velocities and density as shown in Fig. 7.

Another widely used method for calculating synthetic seismograms for a layered medium is the reflectivity method in which the wave-number integral is replaced by a finite sum over discrete wave-numbers. Fuchs [5] was the first to use this method in 1968 for modeling body waves by summing over the homogeneous plane waves. The method was later extended to include inhomogeneous plane waves [6], [7]. The singularities corresponding to surface wave poles are removed by introducing a small imaginary part ω' to frequency ω, and the effect was later removed by multiplying the final time-domain solution by $e^{\omega' t}$. The resultant synthetic seismogram is exact up to the time when the first signal arrives from the nearest of the spurious sources aligned at the interval $1/(\Delta k)$, where Δk is the discrete wave-number interval. The method, therefore, is most effective for near-source problems. Figure 8 shows the horizontal component displacement perpendicular to the fault strike generated by a propagation of strike-slip motion in a layered medium calculated by Bouchon [8]. This calculation involves a fivefold integral; ω, k_x, k_y, and areal integration over the fault plane. The areal integral was done first analytically, and then the remaining three integrals were replaced by the discrete sums. The computed displacement simulates well the actual record obtained during the Parkfield earthquake of 1966. As

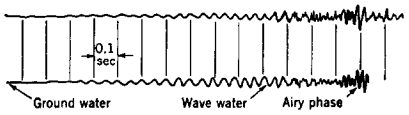

FIG. 3. Ground wave and water wave (through two different filters) from an explosive charge of 55 lb observed at a range of 1030 times water depth (90 ft). Source and receiver in water. Reproduced from [1].

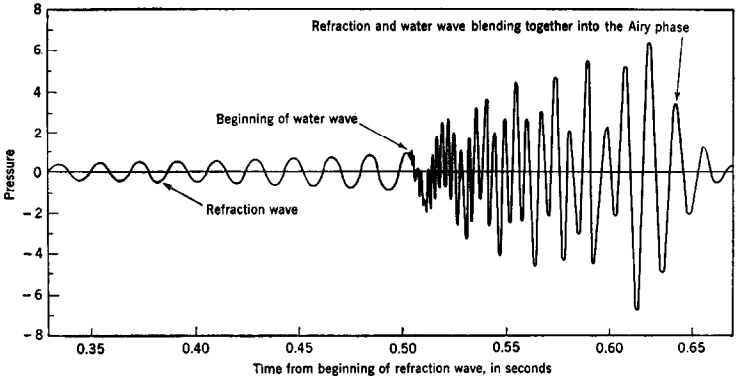

FIG. 4. Theoretical wave motion in first mode for range 460 times water depth (60 ft) calculated by Pekeris [2]. Reproduced from [1].

shown in Fig. 8, one can identify the arrivals of shock waves and their reflections in the synthetic seismogram.

The same method can be used to calculate seismograms to considerable distances within the capability of present-day computers. For example, according to Bouchon (personal communication), seismograms at an epicentral distance 300 km for a strike-slip earthquake in a three-layer crust over a homogeneous mantle can be calculated in 27 min (CPU time) from the first arrival to the end of the *S*-wave group (total length 100 sec). The Nyquist frequency was 5 Hz, the number of frequency points is 512, and the number of wave-number points for each frequency is up to 1000 depending

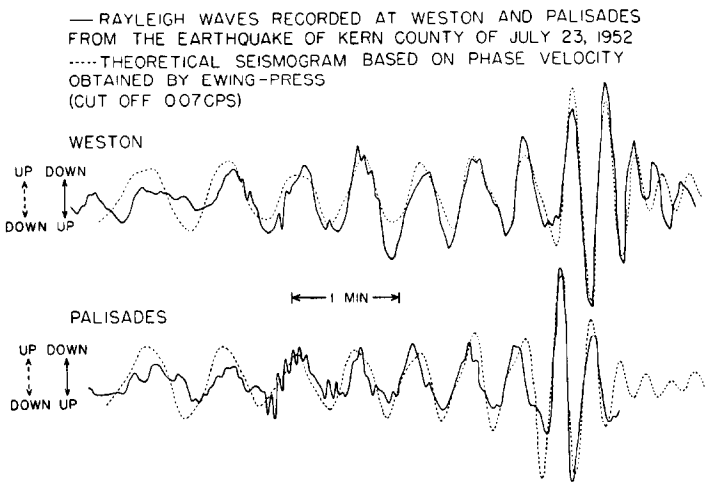

FIG. 5. Theoretical seismograms (dashed line) of Rayleigh waves for the wave paths from Kern County, California to Weston, Mass. and Palisades, N.Y. compared with the actual seismograms (solid line). Reproduced from [3].

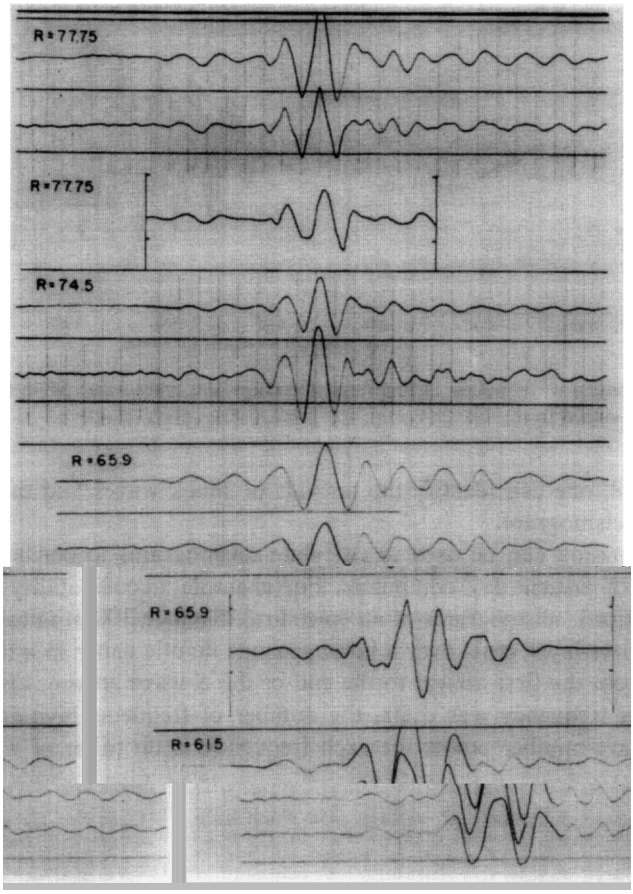

FIG. 6. Comparison of observed seismograms (with vertical time lines) in the Bering Sea at distances 77.75, 65.9, and 61.5 km with synthetic seismograms (without time line) computed for the model shown in Fig. 7. Reproduced from [4].

on frequency. The resultant seismogram was quite similar in general appearance to the observed one in Central Massif, France, for which the modeling was intended. The agreement is, however, only in the general appearance. The details of wave-form do not match between the observed and the synthetic. Even if one can get a good match in detail for a particular observation point by modifying the structure, the same structure will not explain the observed seismogram at another observation point a few kilometers away. Short-period waves cannot be modeled exactly by a 1-D structure.

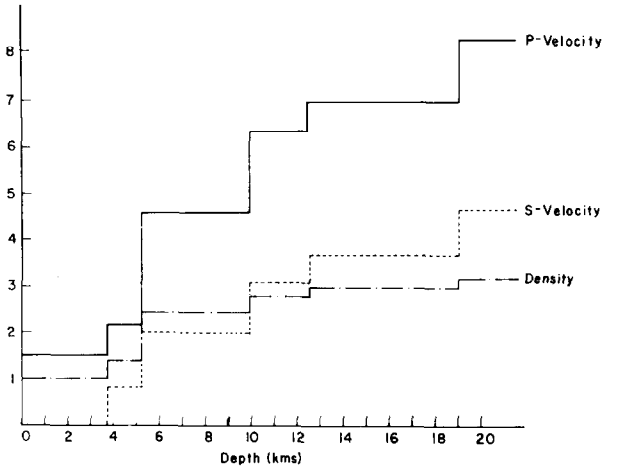

FIG. 7. The distribution of P wave velocity, S wave velocity, and density with depth used for computing the synthetic seismogram shown in Fig. 6. Reproduced from [4].

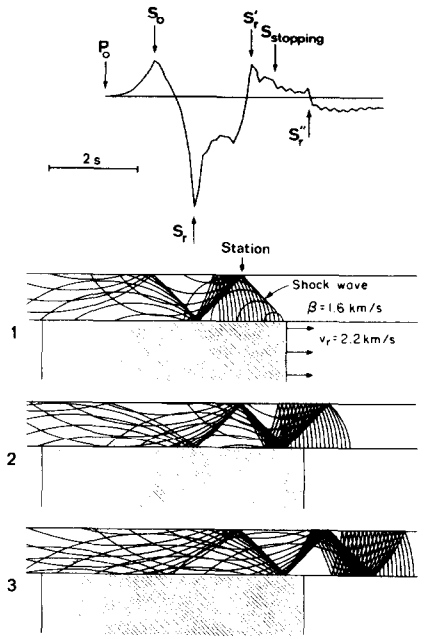

FIG. 8. Top: seismic displacement near a fault in the horizontal direction perpendicular to the fault strike predicted for a strike slip fault simulating the Parkfield earthquake of 1966. Lower figures illustrate the wavefronts in the low velocity (shear velocity 1.6 km/s) layer at the times of the arrivals of (1), S_r, (2) S_r', and (3) S_r''. Shaded area is the fault plane extended toward the right with a rupture velocity of 2.2 km/sec. Reproduced from [8].

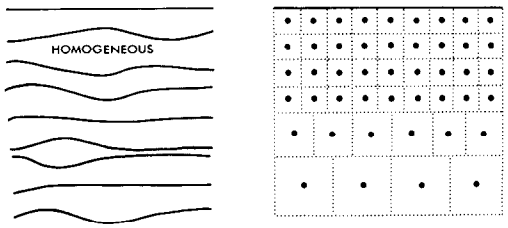

FIG. 9. Two ways of perturbing horizontally layered media (3-D models). On the left, the velocity in each layer is kept uniform, but the interface shape is changed from horizontal. On the right, the interface is kept horizontal, but the layer is divided into blocks with different velocities or the velocity is interpolated from the values assigned at the mesh points.

HOW TO MODEL 3-D EARTH'S STRUCTURES

The accumulating data in the past decades demanded a more flexible model than a 1-D model, but they were not sufficient for a unique determination of the general 3-D model. Two natural approaches are illustrated in Fig. 9. One is perturbation of layer thickness for a stack of homogeneous layers. The other is the perturbation of velocity of seismic waves either by specifying the perturbation at mesh points (the velocity at an arbitrary point is interpolated from the values at mesh points) or by assigning a homogeneous velocity perturbation to blocks into which the medium is divided.

An example of the layer-thickness perturbation model is shown in Fig. 10. It is a problem of *SH* waves vertically incident upon a basin structure filled with low-velocity sediment studied by Boore [9]. The basin has the shape of a full-cycle cosine with wave-length 5 km (because of symmetry only the right half of the body is shown) and 600 m deep at the deepest point. The shear velocity in the half-space is 3.5 km/sec, five times higher than the sediment velocity. Figure 10 compares the result of the finite-difference method (solid line) with the flat layer approximation (dashed line) commonly used in engineering seismology. Figure 11 shows synthetic seismograms computed by various methods for the same problem, but the time and distance scale are both 10 times greater than those in Fig. 10. The *SH*-displacement is computed at equal intervals from the center of the basin (0 km) to a horizontal distance of 20 km. This figure is adapted from Hong and Helmberger [10] to include the results obtained by Bard–Bouchon's method of discrete wave-number [11].

3-D INVERSION OF THE TRAVEL TIME DATA OBTAINED BY 2-D ARRAY OF SEISMOGRAPHS

The velocity-perturbation block model, on the other hand, has been most useful for inverting the travel time data obtained at seismic arrays spread over the Earth's surface into 3-D seismic structure of the Earth's interior.

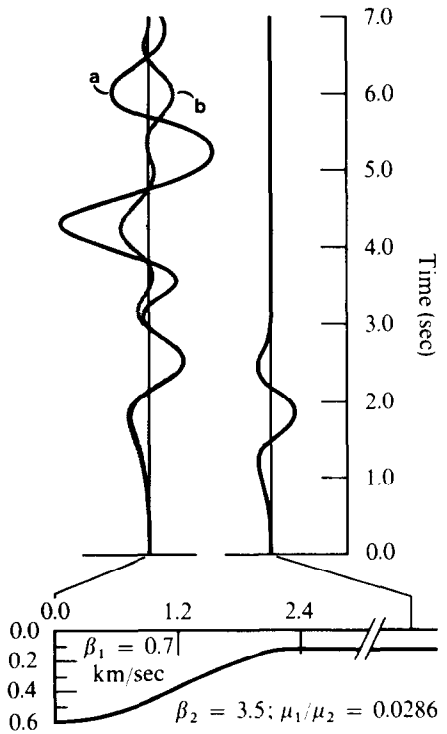

FIG. 10. Seismic motion at the surface of a basin structure due to vertically incident *SH*-waves. Comparison of the finite-difference result (a) with the flat layer approximation (b). Adapted from [9].

The inversion procedure was first applied to the teleseismic data obtained at the NORSAR array in Southern Norway by Aki, Christoffersson, and Husebye [12]. Our basic idea was the following. We measure travel times of body waves at individual stations of an array for many distant earthquakes occurring around the world. We subtract from the observed time the predicted time for each source-reciever using the initial models of earthquake source parameters and the Earth's structure. This residual is the basic data for the inversion procedure. We then divide the Earth beneath the array into several layers and each layer into many blocks.

For each of the blocks we assign an unknown parameter which describes the deviation of the seismic velocity in the block from the average velocity of the layer to which the block belongs. We then set up a large set of equations which relate the observed residuals with the unknown velocity parameters. Typically, the number of observed residuals is a few thousand and the number of unknowns is a few hundred. The solution was obtained by the method of generalized inverse [13] or the method of stochastic inverse [14].

The method was refined by Ellsworth [15] who incorporated 3-D ray tracing and repeated the linearization procedure. In most cases of teleseismic data, the result without iteration was close to the one obtained by iteration.

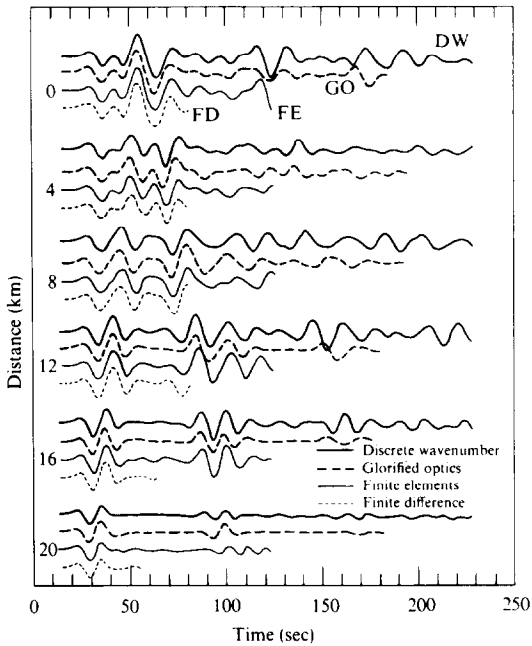

FIG. 11. Synthetic seismograms computed by various methods for motions on the surface of a basin structure due to *SH*-waves impinging vertically from the half-space. The shape of the basin and the velocities are identical to those shown in Fig. 10. The only difference is in scale; the time and distance scales are both 10 times greater than those in Fig. 10. The *SH*-displacement is computed at equal intervals from the center of the basin (0 km) to a horizontal distance of 20 km. This figure is reproduced from [11]. This is adapted from [10] to include the results obtained by the discrete wave number (DW) method.

The method was extended to local earthquake data by Aki and Lee [16] who assumed a homogeneous initial model and applied it to the data from Bear Valley, Calif. In this case, because of the sensitivity of shorter period waves to smaller scale heterogeneity, several steps of linearization-iteration are needed. Various 3-D ray tracing methods [17] and approximate methods [18, 19] have been developed specifically for this purpose.

In the case of local earthquake data, their locations and origin times are also unknowns. However, it was shown by Pavlis and Booker [20] and Spencer and Gubbin [21] that the source parameters can be eliminated from the equation for the velocity parameters.

So far the method has been applied to 24 arrays around the world with the aperture ranging from 20 to 2000 km. With a larger aperture array, a deeper structure can be studied. On the other hand, the details will be lost because the station spacing tends to become greater for a larger aperture array.

Some of the highlights of the results are (1) the confirmation of a down-going Pacific plate under Japan [22], (2) the detailed picture of the subduction of the

Philippine Sea plate with the suggestion of a collision boundary for the Izu Peninsula [23], (3) low velocity bodies in the crust and upper mantle associated with geothermal areas in the western U.S. [24–27], (4) discovery of a low velocity zone under central California dipping toward the east [28] and a strong anomaly in the asthenosphere under southern California [29], (5) detailed 3-D structure of the San Andreas and neighboring fault zone [27, 30], and (6) evidence for the subduction of continental crust in Hindu Kush [31].

Two approaches have been used for the linearization-iteration procedure in our inverse problem. We assume that data vector d is a function of model vector m plus noise n.

$$d = f(m) + n. \tag{4}$$

Assuming that the noise is Gaussian with the covariance matrix R_n, and that the model is also Gaussian with the mean equal to the initial model m_0 and the covariance matrix R_m. Then, the stochastic inverse solution is given by the minimization of

$$(d - f_\kappa(m))^T R_n^{-1}(d - f_\kappa(m)) + (m - m_0)^T R_m^{-1}(m - m_0), \tag{5}$$

where

$$f_\kappa(m) = f(m_{\kappa-1}) + f(m_{\kappa-1})(m - m_{\kappa-1}),$$

at the κth linearization-iteration step as given by Jackson [32] and Tarantola and Vallete [33].

This is different from the usual Newtonian approach. We usually consider the revised solution as the new initial model and minimize

$$(d - f_\kappa(m))^T R_n^{-1}(d - f_\kappa(m)) + (m - m_{\kappa-1})^T R_m^{-1}(m - m_{\kappa-1}). \tag{6}$$

In this case, the solution can wander away in the model space as the iteration proceeds. We can, however, get a reasonable solution if we stop the iteration as soon as the variance reduction becomes statistically insignificant. The significance may be tested by the F test on the variance reduction. This scheme seems to work well, but the approach based on Eq. (5) appears to be more logical from the point of the stochastic inverse.

Statistical Approach in Modeling the Earth's Structure

So far we have described deterministic models of the Earth's structure. The deterministic approach becomes increasingly difficult as the period of seismic waves under study becomes shorter. The shorter period waves suffer from scattering by smaller scale heterogeneities which do not affect longer waves. Since small scale heterogeneities require a large number of parameters for their complete description,

we need a large number of observations to determine them. When the observations are limited, we must resort to a statistical model which can describe the statistical property of the Earth's structure with a smaller number of parameters.

The statistical approach can be divided into two major branches; namely the forward scattering and backward scattering. As an example of the forward scattering approach, we mention the fluctuation of amplitude and phase of teleseismic P wave across the Montana LASA array studied using Chernov's [34] theory of random medium by Aki [35] and Capon [36]. They found from the observations in the frequency range 0.5 to 1.0 Hz that the lithosphere under LASA can be characterized by a random medium with the correlation distance of 10 km and the RMS velocity fluctuation of a few percent.

On the other hand, the back-scattered waves can be found in the later part of a local earthquake seismogram recorded at a short distance from the source after the passage of all the primary waves. The later part of a local earthquake seismogram is called coda waves, and we now believe that they are primarily S waves scattered back from heterogeneities which are more or less uniformly distributed throughout the lithosphere. The idea of attributing coda waves to back-scattering was first proposed by Aki [37] based on the data from central California. The study was extended to Japan [38, 39], the U.S.S.R. [40], and various other areas. The evidences for the S to S back-scattering [41, 42] are the following.

(1) Coda and S waves share the same Q value for a wide frequency range (1-25 Hz). [40–43].

(2) Coda and S waves share the same site-effect for the above frequency range [39].

(3) Similarity of general nature of coda waves between surface and deep bore hole (~3 km) sites in Japan, excluding the surface wave scattering, at least there.

Using a single scattering theory, the power spectrum of coda waves $P(\omega \mid t)$ at a lapse time t measured from the origin time of earthquake can be written as [38, 41],

$$P(\omega \mid t) = \frac{\beta}{2} g(\pi) \mid S(\omega) \mid^2 \left(\frac{\beta t}{2}\right)^{-2} e^{-\omega t/Q_c}, \tag{7}$$

where β is the shear wave velocity, $S(\omega)$ is the source spectrum for shear waves, Q_c is the Q for coda waves, and $g(\pi)$ is the back-scattering coefficient [$g(\theta)$ is the differential scattering coefficient in the direction making an angle θ with the propagation direction of primary waves].

Equation (7) has been used for studying the source spectra of earthquakes, and attenuation and scattering properties of high-frequency shear waves for various regions of the Earth.

Recently, Sato [43] summarized the observations on Q of S and coda waves as shown in Fig. 12 for the frequency range from 1 to 25 Hz. The figure also shows the Q of shear waves in the lithosphere at long periods inferred from the attenuation of

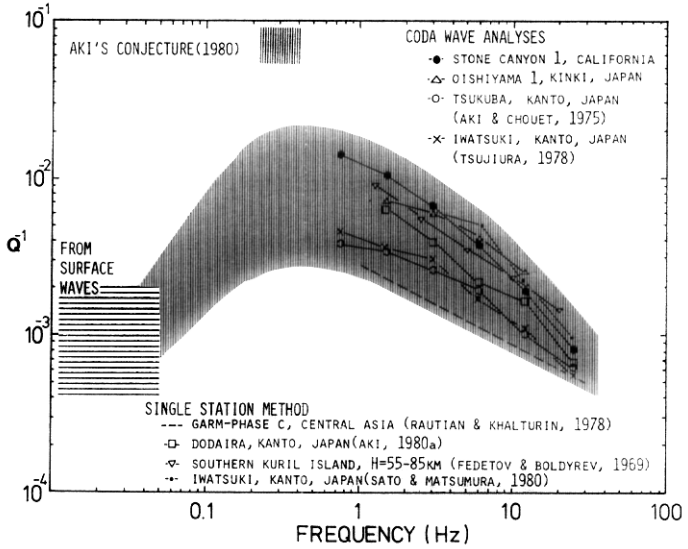

FIG. 12. Frequency dependence of $Q - 1$ for shear waves in the lithosphere, reproduced from [43].

Love and Rayleigh waves with periods longer than about 20 sec. Since the surface

area from which Q for frequencies higher than 1 Hz has been obtained, the two data sets may not be combined simple-mindedly. But, in view of the ubiquity of the increase in Q^{-1} with decreasing frequency for the range form 1 to 25 Hz and the universally high Q value associated with the surface waves with period of 20 sec, it is reasonable to conjecture that Q^{-1} has a peak near 1 Hz as indicated in Fig. 12.

We have been searching for the attenuation mechanism that would explain the frequency dependence of Q^{-1} as shown in Fig. 12. At present, the most promising mechanism appears to be the loss of energy by scattering due to heterogeneity.

CONCLUSION

We may summarize the status of short-period seismology by saying that we are in a transition period from the 1-D Earth model to the 3-D model. For the 1-D model, we have well-established theory and methods such as Cagniard–DeHoop and reflectivity or discrete wave number (see [11, Chap. 9]).

For the 3-D model, the method for handling the travel time data using the ray tracing seems to be well developed for both forward and inverse problems. The methods for computing wave forms and spectra in 3-D models are, however, in a rudimentary stage (see [11, Chap. 13]).

Stochastic approaches in Earth structure modeling are useful particularly for short period waves for which the data are usually not sufficient for a deterministic interpretation.

ACKNOWLEDGMENT

This material is based upon work supported, in part, by the National Science Foundation under Grant PFR 8005720.

REFERENCES

1. M. EWING, W. JARDETSKY, AND F. PRESS, "Elastic Waves in Layered Media," McGraw–Hill, New York, 1957.
2. C. L. PEKERIS, *Geol. Soc. Amer. Mem.* **27** (1948).
3. K. AKI, *J. Geophys. Res.* **65** (1960), 729.
4. D. V. HELMBERGER, *Bull. Seismol. Soc. Amer.* **58** (1968), 179.
5. K. FUCHS, *J. Phys. Earth* **16** (1968), 27.
6. M. BOUCHON AND K. AKI, *Bull. Seismol. Soc. Amer.* **67** (1977), 259.
7. M. BOUCHON, *J. Geophys. Res.* **84** (1979), 3609.
8. M. BOUCHON, *J. Geophys. Res.* **84** (1979), 6149.
9. D. M. BOORE, Finite difference methods for seismic wave propagation in heterogeneous materials, *in* "Seismology: Surface Waves and Earthquake Oscillations" (B. A. Bolt, Ed.), Methods in Computational Physics, Vol. II, Academic Press, New York, 1972.
10. T. L. HONG AND D. V. HELMBERGER, *Bull. Seismol. Soc. Amer.* **68** (1978), 1313.
11. K. AKI AND P. G. RICHARDS, "Quantitative Seismology: Theory and Methods," 2 vols. Freeman, San Francisco, 1980.
12. K. AKI, A. CHRISTOFFERSSON, AND E. S. HUSEBYE, *J. Geophys. Res.* **82** (1977), 277.
13. C. LANCZOS, "Linear Differential Operators," Van Nostrand, London, 1961.
14. J. N. FRANKLIN, *J. Math. Analysis Appl.* **31** (1970), 682.
15. W. L. ELLSWORTH, "Three-Dimensional Structure of the Crust and Mantle Beneath the Island of Hawaii," Ph.D. thesis, MIT Press, Cambridge, Mass., 1977.
16. K. AKI AND W. H. K. LEE, *J. Geophys. Res.* **81** (1976), 4381.
17. J. P. YANG AND W. H. K. LEE, "Preliminary investigations of computational methods for solving the two-point seismic ray-tracing problem in a heterogeneous and isotopic medium," U.S. Geological Survey Open-file Report, 76-707, 1976.
18. A. HORIE, "Three Dimensional Seismic Velocity Structure beneath the Kanto District by Inversion of *P*-Wave Arrival Time," Ph.D. thesis, Univ. of Tokyo, 1980.
19. C. H. THURBER AND W. L. ELLSWORTH, *Bull. Seismol. Soc. Amer.* **70** (1980), 1137.
20. G. L. PAVLIS AND J. R. BOOKER, The mixed discrete-continuous inverse problem. Application to the simultaneous determination of earthquake hypocenters and velocity structure, *J. Geophys. Res.*, in press.
21. C. SPENCER AND D. GUBBIN, *Geophys. J. Roy. Astron. Soc.* **63** (1980), 95.
22. K. HIRAHARA, *J. Phys. Earth* **25** (1977), 393.
23. K. HIRAHARA, Three-dimensional seismic structure beneath southwest Japan—The subducting Philippine sea plate, *Tectonophysics*, in press.
24. H. M. IYER, D. H. OPPENHEIMER, AND T. HITCHCOCK, *Science* **204** (1979), 495.
25. P. REASENBERG, W. L. ELLSWORTH, AND A. WALTER, *J. Geophys. Res.* **85** (1980), 2471.
26. R. ROBINSON AND H. M. IYER, Delineation of a low-velocity body under the Roosevelt Hot Springs geothermal area, Utah, using teleseismic *P* wave data, *Geophysics*, in press.

27. G. ZANDT, "Study of Three-Dimensional Heterogeneity beneath Seismic Arrays in Central California and Yellowstone, Wyoming," Ph.D. thesis, MIT Press, Cambridge, Mass., 1978.
28. R. COCKERHAM AND W. L. ELLSWORTH, *Trans. Amer. Geophys. Union* **60** (1979), 875.
29. S. A. RAIKE, *Geophys. J. Roy. Astr. Soc.* **63** (1980), 187.
30. C. H. THURBER, "Earth Structure and Earthquake Locations in the Coyote Lake Area, Central California," Ph.D. thesis, MIT Press, Cambridge, Mass., 1981.
31. S. W. ROECKER, "Seismicity and Tectonics of the Pamir-Hindu Kush Region of Central Asia," Ph.D. thesis, MIT Press, Cambridge, Mass., 1981.
32. D. D. JACKSON, *Geophys. J. Roy. Astron. Soc.* **57** (1979), 137.
33. A. TARANTOLA AND B. VALETTE, Inverse problems: Quest of information, *Geophys. J. Roy. Astron. Soc.*, in press.
34. L. A. CHERNOV, "Wave Propagation in a Random Medium," McGraw–Hill, New York, 1960.
35. K. AKI, *J. Geophys. Res.* **78** (1973), 1334.
36. J. CAPON, *Bull. Seismol. Soc. Amer.* **64** (1974), 235.
37. K. AKI, *J. Geophys. Res.* **74** (1969), 615.
38. K. AKI AND B. CHOUET, *J. Geophys. Res.* **80** (1975), 3322.
39. M. TSUJIURA, *Bull. Earthquake Res. Inst., Univ. Tokyo* **53** (1978), 1.
40. T. G. RAUTIAN AND V. I. KHALTURIN, *Bull. Seismol. Soc. Amer.* **68** (1978), 923.
41. K. AKI, *J. Geophys. Res.* **85** (1980), 6496.
42. K. AKI, *in* "Proceedings of the NATO Advanced Study Institute on Identification of Seismic Sources," pp. 8–18, Oslo, Norway, September, 1980.
43. H. SATO, *in* "IASPEI Symposium on Heterogeneities of the Lithosphere," London, West Ontario, July, 1981.
44. S. A. FEDOTOV AND S. A. BOLDYREV, *Izv. Acad. Sci. USSR (Phys. Solid Earth)* **9** (1962), 17.
45. H. SATO AND S. MATSUMURA, *Jishin, J. Seismol. Soc. Japan* (2) **33** (1980), 541.